

U. S. DEPARTMENT OF COMMERCE  
NATIONAL OCEANIC AND ATMOSPHERIC ADMINISTRATION  
NATIONAL WEATHER SERVICE  
NATIONAL METEOROLOGICAL CENTER

OFFICE NOTE 91

Diagnosis of Noise in the NMC Global Model Using a Time Filter

Ronald D. McPherson  
Robert E. Kistler  
Clifford H. Dey  
Development Division

JANUARY 1974

## DIAGNOSIS OF NOISE IN THE NMC GLOBAL MODEL USING A TIME FILTER

### I. Introduction

A preliminary description of the noise oscillations in the NMC 8L GLOBAL model has been given in an earlier Office Note (McPherson and Stackpole, 1973). By examining the temporal behavior of pressure and height variables at individual grid points, three significant components of the noise were identified on the basis of differences in amplitude and period. One has small amplitude (5-10 m) and short period (2-3 hours), another has larger amplitude (10-25 m) and longer period (6-7 hours), and the third possesses an amplitude ranging from 20 to 40 m and a period of approximately 10-14 hours. All three were described as external gravity modes, since their phases did not vary with height, at least through 300 mb.

The present note reports on a continuation of the earlier study and represents both new experiments and reinterpretation of some aspects of the earlier study. Our intent is to supply a quantitative estimate of the magnitude of the noise, as well as additional information on its characteristics. We have approached the problem by using a time filter to isolate the noise. The design and response of the filter are described in the next section.

### II. Filter Design and Response

The design of the filter is based on the assumption that all oscillations with periods shorter than about 12 hours are noise, while

oscillations of meteorological interest on the global scale possess periods greater than 24 hours. Therefore, the desired response of the filter is near zero for periods less than 12 hours and near unity for periods greater than 24 hours. A brief summary of the theory of filter design follows.

If  $x_j$ ,  $j=0, J$ , represents a time sequence of evenly-spaced observations, and  $x_n$  represents the nth value of  $x$  at time  $t = t\Delta t$ , then a filtered value of  $x_n$  may be written as

$$f_n = \frac{1}{2} \sum_{m=0}^M w_m (x_n + m + x_n - m) \quad (1)$$

where the  $w_m$  are a set of weights which will be referred to as the "filter." Assuming that  $x_n$  is representable as a cosine function,

$$x_n = A \cos \left[ \frac{2\pi n \Delta t}{T \Delta t} + \phi \right] \quad (2)$$

where  $T \Delta t$  is the period, and  $\phi$  is a phase shift, we can replace the  $x$ 's in equation (1) to obtain

$$f_n = \frac{1}{2} \sum_{m=0}^M w_m \left\{ A \cos \left( \frac{2\pi(n+m)}{T} + \phi \right) + A \cos \left( \frac{2\pi(n-m)}{T} + \phi \right) \right\} \quad (3)$$

Using trigonometric identities, equation (3) can be reduced to

$$f_n = A \cos\left(\frac{2\pi n}{T} + \phi\right) \sum_{m=0}^M w_m \cos\left(\frac{2\pi m}{T}\right). \quad (4)$$

But the expression multiplying the summation in equation (4) is just  $x_n$ , by equation (2); therefore

$$\frac{f_n}{x_n} = \sum_{m=0}^M w_m \cos\left(\frac{2\pi m}{T}\right) \equiv R, \quad (5)$$

where the ratio of filtered to unfiltered values is defined as  $R$ , the response of the filter for waves of period  $T\Delta t$ . It is then possible to design a filter by specifying desired responses for  $M + 1$  different  $T$ 's, thus giving  $M + 1$  equations in  $M + 1$  unknown weights,  $w_m$ .

After considerable experimentation with different combinations of response specifications, we arrived at a 21-point filter which possesses most of the desired attributes. The filter is given below.

$$w_0 = 0.14961 \quad w_6 = 0.01705$$

$$w_1 = 0.29004 \quad w_7 = 0.00484$$

$$w_2 = 0.23703 \quad w_8 = 0.00815$$

$$w_3 = 0.17205 \quad w_9 = 0.00538$$

$$w_4 = 0.10854 \quad w_{10} = 0.00408$$

$$w_5 = 0.04813$$

The response function for this filter is illustrated in two ways in Figure 1. The upper graph displays the response on the ordinate plotted against the frequency on the primary abscissa and the period on the secondary abscissa. The lower graph shows the response as a function of period on a linear scale.

All waves of periods 6 hours and less are reduced to less than 0.1 percent of their original amplitudes, waves of 10-hour periods are reduced to 25 percent, and waves with periods of 30 hours and longer retain more than 90 percent of their original amplitude. It is likely that further experimentation would have produced sharper response characteristics, but this filter appears to be adequate for our purposes.

### III. Application of the Filter

The global model was first integrated to 24 hours on a  $5^{\circ}$  grid mesh. Hourly values of the history variables (except moisture) at each grid point and  $\sigma$ -level were stored on tape. Next, the hourly values of the u- and v- components, the pressure thicknesses, and the potential temperatures for each grid point from the second through the 22nd hour were multiplied by the weight appropriate to each hour and the results summed as in equation (1). The result is a filtered value of each variable at all grid points, valid at the 12th hour. These fields will be referred to in subsequent discussions as "filtered forecasts." In principle, they are not contaminated by the presence of high-frequency noise. We may, therefore, obtain an estimate of the magnitude and spatial distribution of the noise by comparing the filtered 12th-hour fields with their unfiltered counterparts.

This procedure was applied in two synoptic cases, 0000 GMT, 20 March 1973, and 1200 GMT, 25 March 1973. Root-mean-square (RMS) differences were computed for surface pressure, for wind speed and temperature in each sigma-layer and for the heights of standard pressure levels after interpolation from sigma to pressure coordinates. Both filtered and unfiltered 12-hour forecasts were verified against radiosonde observations at 70 Northern Hemisphere locations. RMS errors of height, temperature, wind speed, and vector wind were tabulated at standard pressure levels.

#### IV. Spatial Distribution of the Noise

Figures 2 and 3 show the difference between filtered and unfiltered tropospheric and stratospheric pressure thicknesses from pole to pole and from 0 to 110W longitude. These difference charts represent the combined effect of all oscillations with periods of 10 hours or less. In the troposphere, the principal component is a very large scale latitudinal variation (two waves from pole to pole). Its amplitude is apparently not large: approximately 2 mb. There are disturbances of larger amplitude but much smaller scale superimposed. The same pattern appears in the stratosphere, but in the opposite phase. Adding the troposphere and stratosphere to the 50-mb thick cap layer (which shows minuscule variations and is therefore omitted) yields the difference in surface pressure (Figure 4). The same large-scale (wave two in latitude) pattern appears, but with smaller amplitude than in either the troposphere or stratosphere. It may, therefore, be concluded that the principal large-scale noise component is an oscillation of internal type between

the two main sigma-domains of the model. The external gravity mode (as in the surface pressure field) emerges as a residual between the out-of-phase oscillations of the two sigma domains.

This external gravity mode is the most obvious oscillation in the height difference maps, shown in Figures 5 and 6. At 500 mb, the wave-two pattern is clear; its amplitude is approximately 10 m. The pattern is not so clear at 100 mb, although a very large scale but small amplitude pattern is evident.

#### V. Magnitude of the Noise

Figures 2-6 indicate that the amplitudes of the large-scale components are not great in the one synoptic case. Tables 1 and 2, presenting RMS differences between the unfiltered and filtered forecasts for both cases, confirm this. The numbers are very small: less than  $0.5^{\circ}$  in temperature,  $3 \text{ msec}^{-1}$  in wind speed, 1 mb in surface pressure, and 11 m in height.

RMS errors of both filtered and unfiltered forecasts are tabulated in Tables 3 and 4. The verification statistics are not significantly different between filtered and unfiltered forecasts of wind and temperature. Height errors are consistently smaller at all levels in both cases for the filtered forecast, but only slightly smaller. For example, at 500 mb in the 20 March case, the filter effected a reduction of only 1.4 m in the height error. Both filtered and unfiltered forecasts began from an initial analysis which had an error of 9.8 m, so the error growth in the 12-hour period was 31.7 m. The reduction of 1.4 m resulting from removing the noise amounts to only about 4 percent of the error growth.

## VI. Summary

The evidence from two synoptic cases viewed in the manner described above suggests that the NMC global model exhibits very large-scale gravitational oscillations of both external and internal character, but with relatively small amplitude. Because of the small amplitude, these oscillations have only minor impact on verification scores.

It seems possible that the amplitudes of these large-scale oscillations could be underestimated by the isolation-by-filter technique applied here, since the principal components are of long period (10-12 hours) and the response of the filter is not perfect for those periods. Nevertheless, the evidence is persuasive that, while the noise demonstrably exists, it is not a major contributor to forecast error.

Table 1

RMS differences between filtered and unfiltered  
12-hour forecasts from 0000 GMT, March 20, 1973

P (mb)	$z$ (m)	$\sigma$ level	T (deg.)	$S$ ( $m/sec^{-1}$ )	$P_s$ (mb)
		-	-	-	0.56
1000	6.5	1	0.24	0.95	
800	6.6	2	0.30	1.09	
700	6.7	3	0.09	1.12	
500	7.0	4	0.09	1.33	
400	7.0	5	0.13	1.67	
300	6.6	6	0.15	1.81	
200	7.4	7	0.32	1.92	
100	10.2	8	0.24	2.79	

Table 2

RMS differences between filtered and unfiltered  
12-hour forecasts from 1200 GMT, March 25, 1973

P (mb)	z (m)	$\sigma$ level	T (deg.)	S (m/sec $^{-1}$ )	P <sub>s</sub> (mb)
		-	-	-	0.58
1000	7.0	1	0.20	1.01	
800	6.8	2	0.11	0.96	
700	7.1	3	0.09	0.99	
500	7.3	4	0.08	0.79	
400	7.2	5	0.11	1.08	
300	7.2	6	0.10	1.39	
200	7.4	7	0.35	1.47	
100	9.4	8	0.22	2.21	

Table 3

RMS errors of filtered (F) and unfiltered (U) 12-hour forecasts from 0000 GMT, March 20, 1973. Verifications against 70 Northern Hemisphere radiosonde stations.

P (mb)	Z (m)		T (deg.)		S (kts)		$\vec{V}$ (kts)	
	F	U	F	U	F	U	F	U
850	34.4	36.2	3.6	3.6	8.8	8.9	13.0	12.9
700	32.8	34.5	2.5	2.6	10.1	10.1	13.5	13.6
500	40.1	41.5	1.9	1.9	10.1	10.0	15.4	15.4
300	52.7	53.7	2.7	2.7	12.2	12.2	18.1	18.3
200	49.7	51.7	3.9	3.9	9.7	10.0	14.4	14.7
100	51.4	55.2	2.5	2.5	13.8	13.4	16.5	16.8

Table 4

RMS errors of filtered (F) and unfiltered (U) 12-hour forecasts from 1200 GMT, March 25, 1973. Verification against 70 Northern Hemisphere RAOB stations.

P (mb)	Z (m)		T (deg.)		S (kts)		$\vec{V}$ (kts)	
	F	U	F	U	F	U	F	U
850	26.1	29.2	3.1	3.0	8.3	8.4	11.8	11.9
700	25.2	29.0	1.7	1.7	6.8	6.8	10.0	10.0
500	30.4	32.5	1.9	1.9	10.8	10.7	14.4	14.4
300	44.8	45.9	3.0	3.0	13.9	14.1	21.1	21.4
200	50.4	52.1	3.4	3.4	14.1	14.4	21.0	21.2
100	42.3	42.9	2.8	2.9	10.5	9.7	13.3	13.6

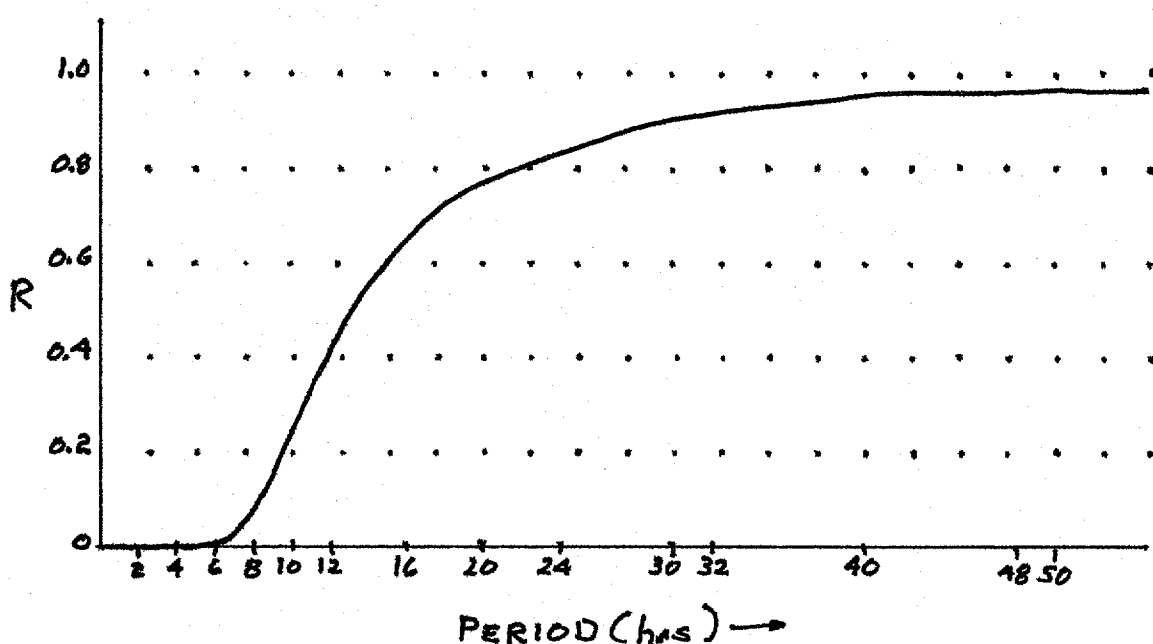
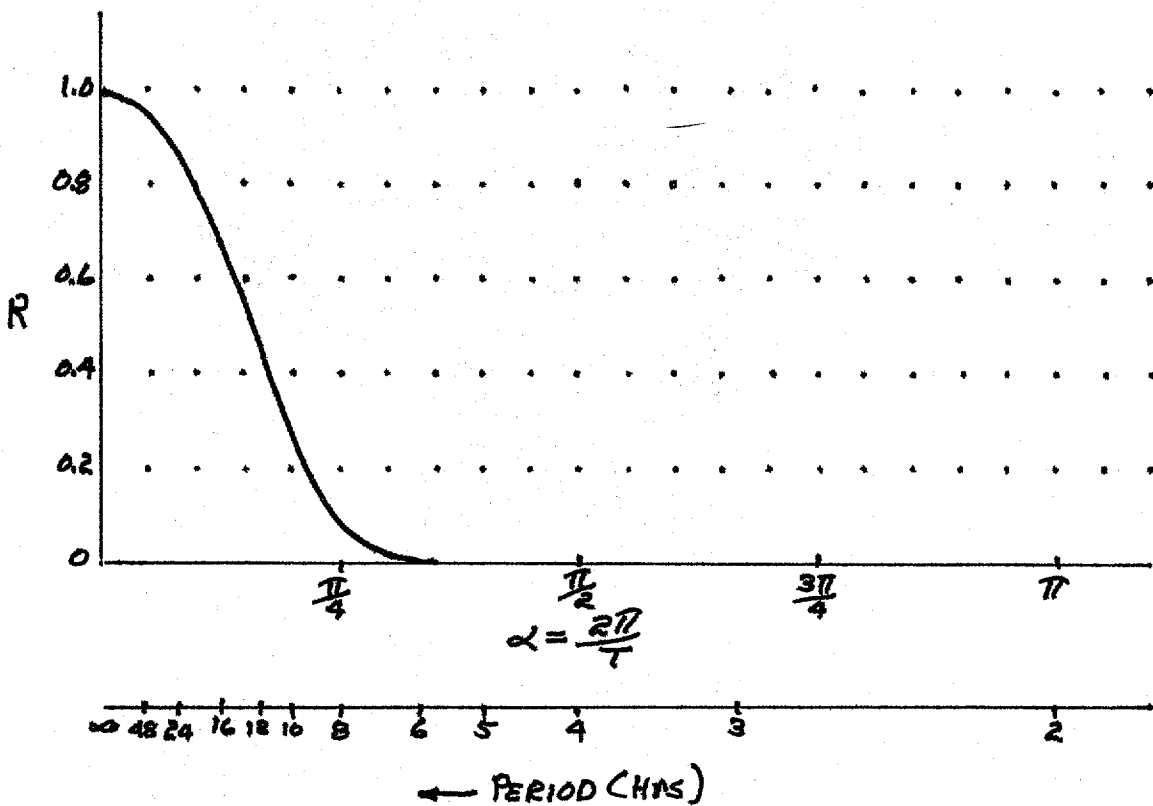


FIGURE 1

2003 MAR 22 1072

Figure 2







